J Fluid Mech (1985), *vol.* 160, *pp* 15–27
Printed in Great Britain

Aerodynamics of slot-film cooling: theory and experiment

By A. D. FITT†,
Department of Engineering Science, Parks Road, Oxford

J. R. OCKENDON
Mathematical Institute, 24–29 St Giles, Oxford

AND T. V. JONES
Department of Engineering Science, Parks Road, Oxford

(Received 13 February 1985)

A simple model is proposed for the two-dimensional injection of irrotational inviscid fluid from a slot into a free stream. In a certain range of values of the ratio of free-stream to injection total heads, the film thickness satisfies a nonlinear integral equation whose solution enables the mass flow in the film to be found. Some experiments are described which both agree with this theory when it is relevant and indicate its deficiencies at other values of the total head ratio

1. Introduction

This paper is concerned with the flow field produced when fluid is injected from a slot into a crossflow. One important physical situation in which this flow field arises is the cooling of gas-turbine blades, where cool gas passes through slots (or holes) onto the blade surface. Effective cooling of the blade enables higher turbine entry temperatures to be employed, which in turn leads to increased power and efficiency The cooling also has to be predictable to some accuracy for Barry (1976) has shown that a variation of 20 °C around a mean blade temperature of 900 °C can halve or double the life of a blade.

The slot-flow field is highly complicated for non-tangential injection, and most research up to the present time has been devoted to experimental studies and semi-empirical models for producing information on the heat-transfer characteristics of a given film cooling system (for a review of earlier work see e.g. Goldstein 1971). Little attention has been given to the details of the velocity field produced by slot injection. The main details of such a flow field for normal injection are shown in figure 1.

In practice the free-stream boundary layer may produce a viscous interaction just ahead of the slot, and there will be a shear layer separating the injected flow and the free stream. The injected flow may separate at the rear of the slot, and subsequently reattach. Downstream of the slot the instability due to the shear layer will cause the flow to become turbulent, and mixing of the free stream and the injected film will occur.

† Present address: Department of Maths and Ballistics, Royal Military College of Science, Shrivenham, Wilts.

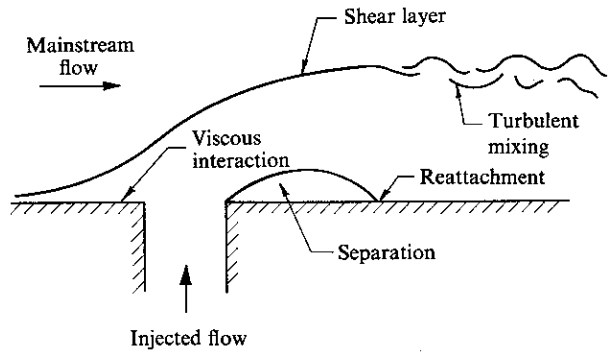

FIGURE 1 A general description of the flow field

In the following analysis the surface viscous boundary layers are assumed to be small compared with the thickness of the injected flow, and the instability of the shear layer is not taken into account. It is also assumed that the flow does not separate at the rear of the slot The free-stream and injected flows are potential flows. The main aim of using these simplifications is to enable a solution to be obtained for the gross influence of the free stream on the injected fluid This influence makes itself felt in the mass-flow–pressure-difference characteristics of the slot The problem of this interaction has not previously been addressed. After a review of known theory, §2 will present a theory for flow from a slot in a certain parameter regime; §3 will describe experimental results.

There are several theories available concerning the injection of incompressible fluid into a free stream with velocity U_∞ and free-stream static pressure p_∞. One theory considers injection through a porous wall aligned with the stream, at injection rates that are small enough for viscous effects to dominate (e.g. Rosenhead 1963; Smith & Stewartson 1973). A rather extreme situation is when the injection is so strong that a large, essentially inviscid, disturbance is produced in the free stream, the simplest example being irrotational injection from a point or line source as in the theory of Rankine solids (Milne-Thomson 1949). In such a limit is it usually tacitly assumed that the total pressure head p_{ti} of the injected fluid is the same as that of the free stream $p_{\mathrm{t}\infty}$. Then no vortex sheet is produced between the two fluids, and the flow field is analytic on the dividing streamline. In two dimensions this enables complex-variable methods to be used, even in quite complicated geometries (Milne-Thomson 1949; Ehrich 1953). However, a wide range of the ratio $p_{\mathrm{ti}}/p_{\mathrm{t}\infty}$ is used in film cooling, and values below $\frac{1}{2}$ are possible For general values of this ratio even an idealized model assuming laminar irrotational flow becomes a complicated free-boundary problem, which can only be solved numerically (Ting & Ruger 1965) Our primary aim in this paper will be to consider flows in which p_{ti} only exceeds p_∞ by a small amount Δp_{t}, since it is in this regime that the influence of the free stream on the injected flow is of paramount importance. This means that the mass flow per unit area from the slot will be much less than that in the free stream and hence that perturbations to the free stream can be treated analytically. To avoid the complexity of viscous boundary layers we will consider Δp_{t} to be not only small compared with $p_{\mathrm{t}\infty}-p_\infty$ but also large enough to ensure that the injected film is thick compared with any viscous boundary layers that may be present. Thus, for example, we assume that the ratio of transverse to tangential velocities in the film greatly exceeds the inverse square root of the local Reynolds number We will also assume that mixing effects

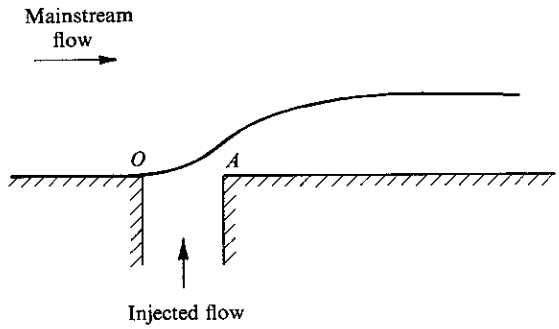

FIGURE 2 The inviscid flow field assumed

resulting from the shear layer are confined to a layer thin compared with the film thickness and that we can assume laminar irrotational flow away from the layer. Some of the experimental evidence in §3 will support these assumptions about the effects of viscosity.

The analysis of §2 will thus concern the flow pattern of figure 2. For simplicity, we neglect separation at the trailing edge of the slot, A; such separation can be minimized in practice by slightly rounding the trailing edge Also we have assumed that the shear layer separates at the leading edge O, although this would not happen in practice because of viscous effects. We conjecture that, because $p_{t\infty} > p_{ti}$, the layer will leave O parallel to the x-axis because only the injectant stream could support a stagnation point at O.

One theory that is directly applicable to figure 2 is the 'inviscid boundary-layer' theory of Cole & Aroesty (1968) They considered the rotational inviscid flow produced by an arbitrary velocity distribution on the straight line OA, solely for the case when v, the normal velocity along OA is proportional to $(\Delta p_t)^{\frac{2}{3}}$ with a suitable non-dimensionalization Indeed, when

$$\left[\frac{v}{U_\infty}\right]^\alpha \propto \frac{\Delta p_t}{p_{t\infty}},$$

where $\alpha < \frac{2}{3}$, it is easy to see that, downstream of the injection region, the film will quickly 'forget' the details of the injection process and adopt an almost-constant velocity and thickness. In such a regime, the free-stream pressure will adjust to that corresponding to flow past a thin aerofoil whose shape is that of the shear layer. However, when $\alpha \geqslant \frac{2}{3}$ the free stream and film interact in the more intimate way described in Cole & Aroesty (1968). We will see in §2 that when the flows in the slot and film are coupled as in figure 2, the film flow is inevitably in the regime of Cole & Aroesty with $\alpha = \frac{2}{3}$. Although our geometry is more complicated than that in Cole & Aroesty, our assumption of irrotationality will make the problem analytically tractable.

2. Small-disturbance theory

Following the discussion in §1, we define a small parameter ϵ by

$$p_{ti} = p_\infty + \tfrac{1}{2}\rho U_\infty^2 \epsilon^2, \tag{1}$$

where ρ is the assumed constant density of the free-stream and injected fluids. In the film downstream of A we expect the pressure to be within $O(\rho U_\infty^2 \epsilon^2)$ of p_∞, and

hence the velocity to be $O(\epsilon U_\infty)$. Now an aerofoil of thickness/chord ratio δ produces free-stream pressure variations $O(\delta\rho U_\infty^2)$, so we also expect the film thickness to be $O(\epsilon^2)$ as $\epsilon \to 0$. Thus the mass flow from the slot $\sim \rho U_\infty \epsilon^3$, which confirms the statement in the introduction that the film flow is in the regime considered by Cole & Aroesty (1968).

We are now in a position to set up dimensionless asymptotic expansions for the velocity potential Φ in the different regions of figure 2. All distances are made dimensionless with the slot width, velocities with U_∞ and pressures with ρU_∞^2.

(i) In the free stream we write

$$\Phi \sim x + \epsilon^2 \phi(x, y) \quad (y > 0, \ -\infty < x < \infty), \tag{2a}$$

where

$$\Delta\phi = 0. \tag{2b}$$

The pressure variation in the outer flow is $-\epsilon^2 \partial\phi/\partial x$ to lowest order, and, if the film thickness is $y \sim \epsilon^2 S(x) + \ldots$, $x > 0$, then

$$\left[\frac{\partial\phi}{\partial y}\right]_{y=0} = \begin{cases} 0 & (x < 0), \\ S'(x) & (x > 0) \end{cases} \tag{3}$$

(ii) In the slot we write

$$\Phi \sim \epsilon^3 \phi_s(x, y) + \ldots \quad (y < 0, \ 0 < x < 1), \tag{4}$$

so that the slot pressure is

$$p \sim \frac{p_\infty}{\rho U_\infty^2} + \tfrac{1}{2}\epsilon^2 + O(\epsilon^6). \tag{5}$$

We now make the important assumption that these orders of magnitude apply all the way upstream to the vortex sheet above the top of the slot. The theoretical reason for this is that we have been unable to find any consistent scaling for small ϵ in which rapid changes occur across the entire slot exit $y = 0$, $0 < x < 1$. For example, if we assume pressure variations across the slot exit comparable to that in the injectant downstream of the slot, a transverse velocity $O(\epsilon)$ is induced in the injectant at the slot exit, and this transverse velocity is so large that it must have zero mean if mass is to be conserved. Hence such pressure variations are only possible if there is an unrealistic region of suction into the slot. Moreover, as we shall see in §3, the experimentally observed pressure variations in the slot are quite gradual except in the vicinity of $y = 0$, $x = 1$, which supports the idea of a 'lid' effect. Thus, to match kinematically with the free stream (2),

$$\frac{\partial\phi_s}{\partial y} = 0 \quad (y = 0, \ 0 < x < 1), \tag{6}$$

but ϕ_s will have a singularity at $(1, 0)$ which is a line sink for the flow from the slot. The precise details of this sink and the flow near $(1, 0)$ are complicated and may depend sensitively on the local geometry, but fortunately we do not need these details to find the film flow downstream.

Matching the pressure with that in the free stream gives

$$\frac{\partial\phi}{\partial x} = -\tfrac{1}{2} \quad (y = 0, \ 0 < x < 1). \tag{7}$$

(iii) In the film downstream of $(1, 0)$, where the irrotational version of the Cole & Aroesty theory applies, the x-component of velocity is ϵu, where, to lowest order,

$$p + \tfrac{1}{2}\epsilon^2 u^2 = \frac{p_\infty}{\rho U_\infty^2} + \tfrac{1}{2}\epsilon^2 \tag{8}$$

Hence, matching the pressure with the free stream,

$$\frac{\partial \phi}{\partial x} = -\tfrac{1}{2} + \tfrac{1}{2}u^2 \quad (y = 0,\ x > 1). \tag{9}$$

However, from conservation of mass

$$uS = \text{constant} = M, \tag{10}$$

which is the unknown scaled dimensionless mass flow out of the slot (for a slot of width d the dimensional mass flow is $\epsilon^3 \rho U_\infty d$). Hence, from (9) and (10),

$$\frac{\partial \phi}{\partial x} = -\frac{1}{2} + \frac{1}{2}\frac{M^2}{S^2} \quad (y = 0,\ x > 1). \tag{11}$$

We have now set the problem up as a nonlinear boundary-value problem for ϕ. Using the fact that the Hilbert transform of $\partial\phi/\partial y$ is $-\partial\phi/\partial x$ on $y = 0$, we may write the equation for S as

$$-\frac{1}{\pi} \int_0^\infty \frac{S'(t)\,\mathrm{d}t}{t-x} = \begin{cases} -\tfrac{1}{2} & (0 < x < 1), \\ -\tfrac{1}{2} + \tfrac{1}{2} M^2/S^2 & (1 < x < \infty). \end{cases} \tag{12}$$

In physical terms, the left-hand side of (12) is effectively the free-stream pressure variation at the dividing streamline caused by a source distribution of strength S'. By momentum conservation across the dividing streamline this pressure variation must equal that in the injectant. A similar approach has been used for cavity problems by Childress (1966).

We expect that $S(0) = S'(0) = 0$ as in figure 2, and that $S = M + O(1/x)$ as $x \to \infty$. This latter estimate is consistent with ϕ behaving logarithmically at infinity, so that $\partial\phi/\partial x = O(1/x)$ on $y = 0$, $x \to \infty$. Moreover, from (12) we expect $S'(x)$ to have a logarithmic singularity at $x = 1$, where, as we have already remarked, our small-disturbance theory is invalid. Finally, and most crucially, we hope that these conditions, together with the continuity of S, which is implicit in (12), will give a unique value for M.

Some numerical evidence for this can be presented by first inverting (12) to give

$$S'(x) = \frac{x^{\frac{1}{2}}}{2\pi} \int_1^\infty \frac{M^2\,\mathrm{d}t}{S^2(t)\, t^{\frac{1}{2}}(t-x)}, \tag{13a}$$

or, if $S = TM^{\frac{2}{3}}$,

$$T'(x) = \frac{x^{\frac{1}{2}}}{2\pi} \int_1^\infty \frac{\mathrm{d}\xi}{T^2(\xi)\, \xi^{\frac{1}{2}}(\xi - x)}. \tag{13b}$$

It is plausible that (13b) has a unique solution for T in $1 < 0 < \infty$ when $T(1)$ is given. If so, for each $T(1)$, this solution may be used to compute T in $0 < x < 1$, and hence to find the continuous solution of (13b) by iterating on the value of $T(1)$. It is easy to show that if T is monotonic and bounded above then the asymptotic estimates

$$T(x) \sim x^{\frac{3}{2}} \quad (x \to 0),$$

$$T(x) \sim T(\infty) - \frac{T^4(\infty)}{\pi x} \quad (x \to \infty)$$

give the behaviour of T at both ends of the range, but it does not seem possible to find $T(\infty)$ analytically. As a consequence of this, we have chosen to find the continuous solution of (13b) numerically, first integrating with respect to x and using the

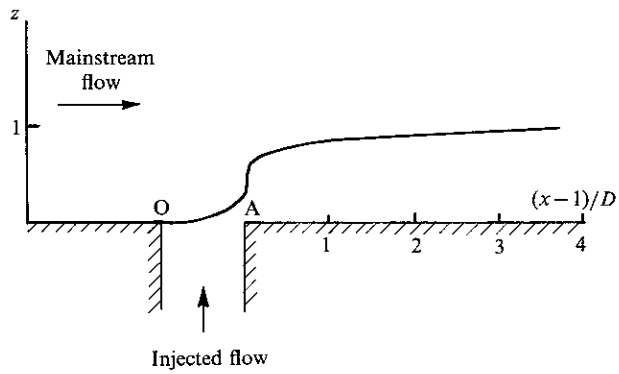

FIGURE 3 The form of the dividing streamline indicated by the analysis

condition $T(0) = 0$ to give

$$T(x) = \frac{1}{2\pi}\int_1^\infty T^{-2}(\xi)\left\{-2\left[\frac{x}{\xi}\right]^{\frac{1}{2}} + \log\frac{\xi^{\frac{1}{2}}+x^{\frac{1}{2}}}{|\xi^{\frac{1}{2}}-x^{\frac{1}{2}}|}\right\}\mathrm{d}\xi, \tag{13c}$$

which is more suitable for numerical calculations as the integral is no longer a principal-value one. We now assume that T is piecewise-constant on the intervals $(\xi_k, \xi_{k+1}]$ $(k = 1, \ldots, N)$ and write

$$2\pi T(x_i) \approx \sum_{k=1}^{N} T^{-2}(\xi_k)\int_{\xi_k}^{\xi_{k+1}}\left\{-2\left[\frac{x_i}{\xi}\right]^{\frac{1}{2}} + \log\frac{\xi^{\frac{1}{2}}+x^{\frac{1}{2}}}{|\xi^{\frac{1}{2}}-x_i^{\frac{1}{2}}|}\right\}\mathrm{d}\xi + E_n \quad (i = 1, \ldots, N), \tag{14}$$

where

$$E_N = \int_{\xi_{N+1}}^\infty T^{-2}(\xi)\left\{-2\left[\frac{x_i}{\xi}\right]^{\frac{1}{2}} + \log\frac{\xi^{\frac{1}{2}}+x^{\frac{1}{2}}}{|\xi^{\frac{1}{2}}-x_i^{\frac{1}{2}}|}\right\}\mathrm{d}\xi.$$

The integral contained in the square brackets may now be explicitly evaluated and the error term E_N may be estimated for large-enough ξ_{N+1} to give the iterative numerical relaxation scheme

$$\left.\begin{aligned} 2\pi\overline{T}_{j+1}(x_i) &= \sum_{k=1}^{n}\left[T_j^{-2}(\xi_k)\,A_{ik}\right] + 2x_i\,T_j^{-2}(\xi_{N+1})\,Q\left(\left(\frac{\xi_{N+1}}{x_i}\right)^{\frac{1}{2}}\right), \\ T_{j+1}(x_i) &= T_j(x_i) + \theta(\overline{T}_{j+1}(x_i) - T_j(x_i)), \quad (i = 1, \ldots, N, j = 1, \ldots), \end{aligned}\right\} \tag{15}$$

where

$$Q(\alpha) = \alpha + \tfrac{1}{2}(1-\alpha^2)\log\frac{\alpha+1}{\alpha-1},$$

$$A_{ik} = 2x_i^{\frac{1}{2}}(\xi_k^{\frac{1}{2}} - \xi_{k+1}^{\frac{1}{2}}) + (\xi_{k+1} - x_i)\log\frac{\xi_{k+1}^{\frac{1}{2}}+x_i^{\frac{1}{2}}}{|\xi_{k+1}^{\frac{1}{2}}+x_i^{\frac{1}{2}}|} - (\xi_k - x_i)\log\frac{\xi_k^{\frac{1}{2}}+x_i^{\frac{1}{2}}}{|\xi_k^{\frac{1}{2}}-x_i^{\frac{1}{2}}|}$$

for the problem on $[1, \infty)$. The solution between 0 and 1 may then be calculated from (14). The sequence of solutions $\{T_j\}$ $(j > 0)$ converged rapidly for all (positive) initial guesses for $T_0(x)$ when the relaxation parameter θ was chosen to be less than 0.1, the calculated value of $T(\infty)$ being 1.04. Thence

$$M = T^3(\infty) = 1.12.$$

The functional form of the solution is shown in figure 3

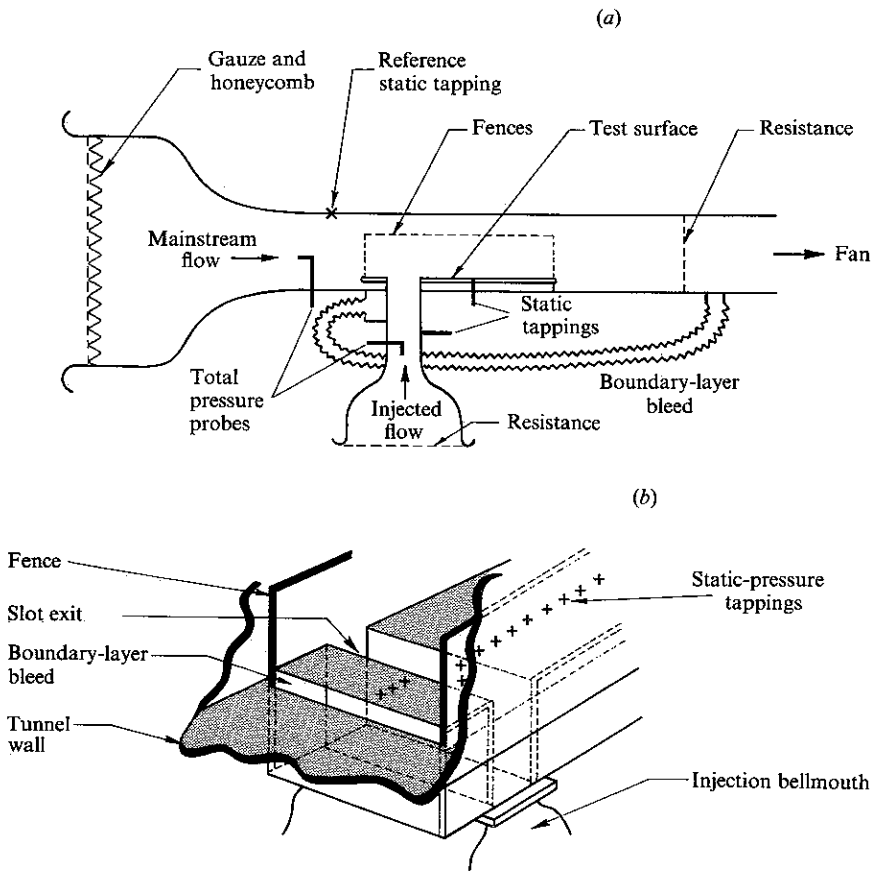

FIGURE 4 (*a*) A schematic diagram of the experiment (*b*) Details of the slot, fences and boundary-layer suction

3. Slot-injection experiments

An open-circuit induced-flow wind tunnel (figure 4) was used to provide the free-stream flow The working-section dimensions were 508 mm × 508 mm, and a 45 kW electrofan exhausted the air to the atmosphere The injected gas was drawn from the atmosphere into the working section through a 40 mm wide slot of aspect ratio 10·1 The air entered the slot via a contraction, and gauze resistances were placed over the entrance to vary the injection total pressure. The tunnel-wall boundary layer was removed by suction 0 1 m from the slot's leading edge The suction was provided by connecting the boundary-layer bleed to the low-pressure region downstream of a resistance placed in the tunnel Care was taken to minimize the sidewall boundary-layer effects by introducing large fences at the point of boundary-layer bleed as shown in figure 4.

Free-stream conditions were found using a Pitot tube in the centre of the tunnel and a wall static measurement. Similarly Pitot and static-pressure measurements enabled the injected flow to be defined, and velocity distributions in the slot were measured. The static pressures along the wall both upstream, downstream and within the slot were also determined Conventional alcohol manometers and an electronic micro-manometer were used for the measurements.

The experiment was run with the slot blanked off and the variation of pressure along the instrumented wall found with respect to a wall static tapping on the opposite wall of the tunnel. This last tapping was used as a reference, for when injection took place, all the static pressures along the instrumented wall varied. Also the zero-injection case enabled wall static-pressure variations resulting from boundary-layer growth on the walls and fences to be evaluated. This last effect was subtracted from the static-pressure variations resulting from injection and was a small correction in the proximity of the slot. For the important measurement of the mass-flow characteristics of the slot the quantity

$$\bar{p} = \frac{p_{\mathrm{ti}} - p_\infty}{p_{\mathrm{t}\infty} - p_\infty}$$

was required. The value of p_∞ was that measured by a wall static tapping nearest to the slot when this was blanked off. The difference between this static pressure and the reference static pressure was small and hence only significant at the lowest injection rates. The free-stream flow velocity was typically 27.4 m/s, giving a slot Reynolds number of 6.5×10^4. The boundary-layer thickness just upstream of the slot in the absence of injection was approximately 4 mm and was essentially turbulent. The injection velocity was measured four slot widths from the slot exit. The boundary layer on the slot walls was small compared with the slot width, and the velocity distribution was uniform. At very low injection velocities the flow became unsteady, and flow uniformity suffered. The injection velocity U_{i} was taken to be the centreline velocity.

The static-pressure distribution along the surface of the plate is shown in figure 5 for several blowing rates $B = U_{\mathrm{i}}/U_\infty$. It can be seen that the general form of the pressure distribution is as expected in that the pressure is sensibly uniform over the slot, but with a large suction peak at the slot trailing edge. The pressure subsequently recovers downstream from the trailing edge. The pressure distribution within the slot is essentially constant for small B and close to the injection total pressure. Upstream of the slot the pressure rises as expected to the slot pressure owing to the injected fluid having the same effect on the external flow as a solid body of the same shape as the film. The form of the pressure distribution downstream from the slot may be predicted from (11), giving

$$\frac{p_{\mathrm{w}} - p_\infty}{\frac{1}{2}\rho U_\infty^2} = B^{\frac{2}{3}}(T_\infty^{-2} - T^{-2}). \tag{16}$$

The pressure distributions are therefore plotted for different injection rates as

$$B^{-\frac{2}{3}} \frac{p_{\mathrm{w}} - p_\infty}{p_{\mathrm{t}\infty} - p_\infty}$$

versus $(x-1)/D$ in figure 6. It can be seen that at the lower injection rates the profile is tending to that expected, and $B^{\frac{2}{3}}$ is a reasonable scaling parameter. As the injection rate is increased, the flow separates from the rear vertex of the slot, and this is clearly seen by the pressure plateau immediately downstream from the slot in figure 5 and 6. The separation was observed using tufts and smoke.

The mass-flow characteristics are shown in figure 7 as B versus the pressure-difference ratio $\bar{p}$. Typical values of $\bar{p}$ lie between 10^{-2} and 1, so that our earlier assumption that the injected film thickness is greater than the viscous-boundary-layer thickness, i.e. that $\bar{p}^{\frac{1}{2}} >$ slot Reynolds number, is justified. The prediction from the present theory is plotted as $B = 1.12\bar{p}^{\frac{3}{2}}$, and in addition the characteristic resulting from the

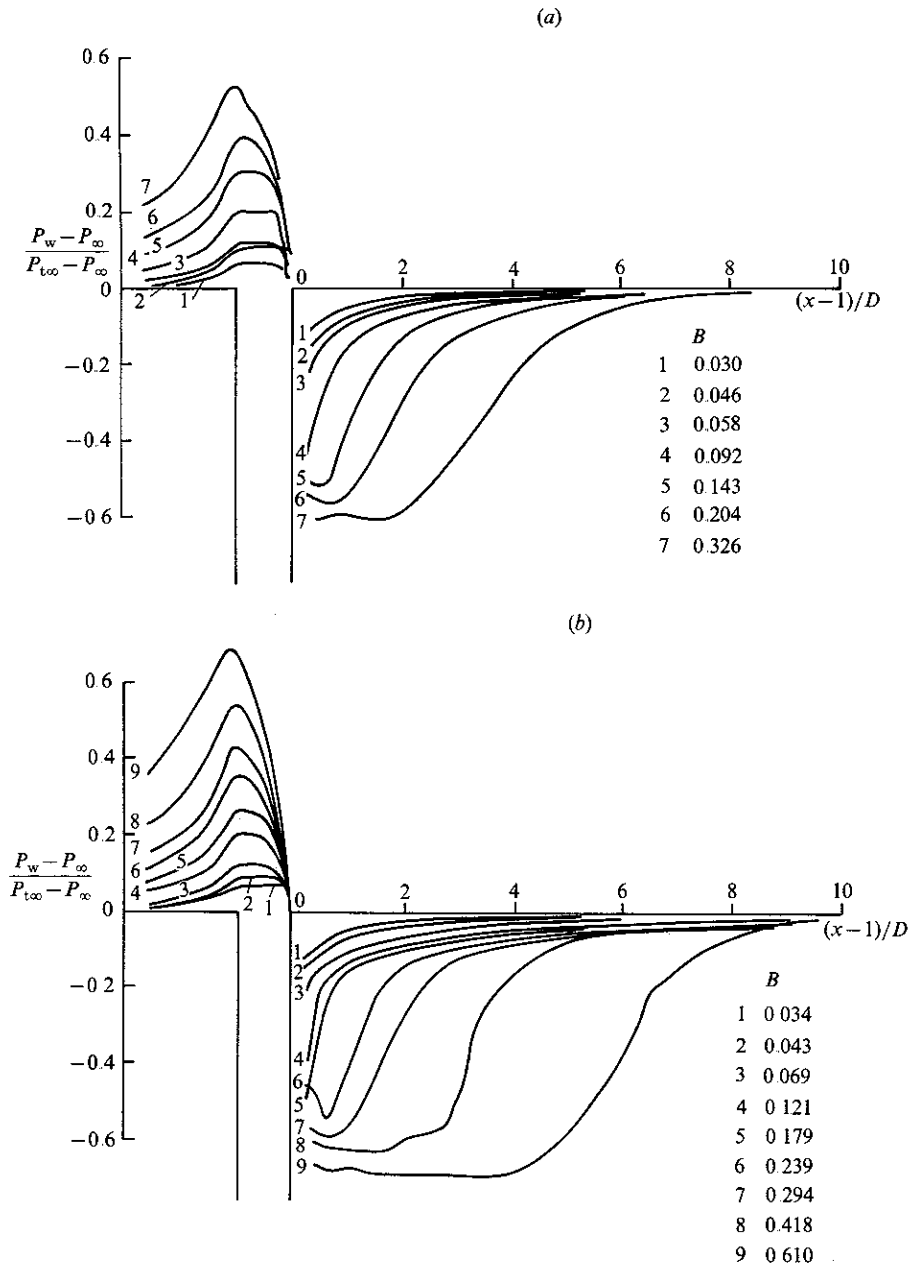

FIGURE 5 (*a*) Normalized static-pressure distributions for (*a*) the slot with sharp trailing edge and (*b*) the slot with a 6 mm radius trailing edge

assumption that the slot exit pressure is the free-stream static pressure is shown as $B = \bar{p}^{\frac{1}{2}}$. Naturally, the latter predicts too high an injection rate, and the prediction $B = (\bar{p} - \frac{1}{2})^{\frac{1}{2}}$, which assumes that the slot exit pressure is the average of the free stream static and total pressures, is also shown It is of interest to plot these results logarithmically as in figure 8, where it can be seen that at the lowest injection rates the injection rate is well above that predicted by the present theory. As the injection rate increases, the results tend to the present prediction and then deviate from this

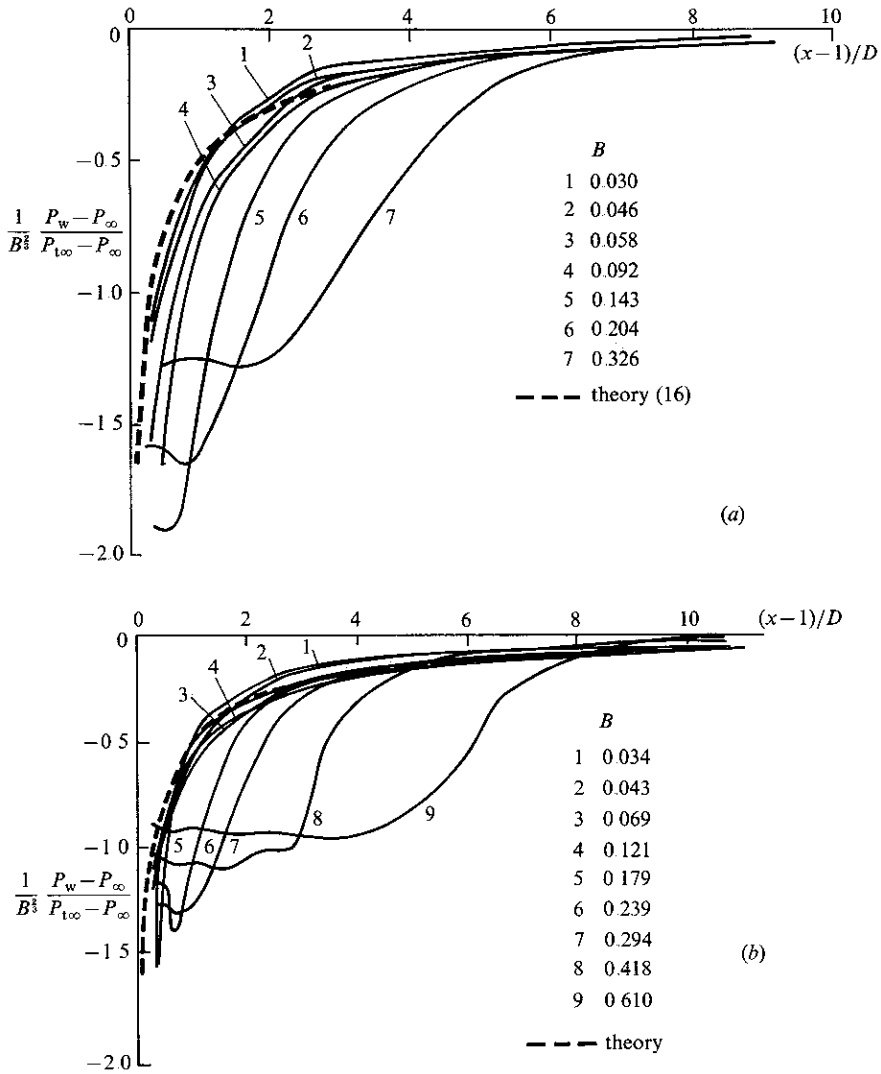

FIGURE 6. $B^{-\frac{2}{3}}(p_w - p_\infty/p_{t\infty} - p_\infty)$ versus $(x-1)/D$ for (*a*) the slot with sharp trailing edge and (*b*) the slot with 6 mm radius trailing edge

as separation becomes important. The differences at the lowest injection rates are understandable, for the boundary-layer thickness is of the same order as the injected layer in this region and viscous effects will become important. A criterion for determining the mass-flow rate at which viscous forces dominate may be roughly estimated by the following argument. If it is assumed that the injected flow rate is very small then the injected–free-stream boundary will become a shear layer downstream from the slot's leading edge. The velocity distribution in a turbulent shear layer is given by Schlichting (1979, p. 738), and when the velocity deficit is U_∞ the injected-fluid volume-flow rate within this shear layer is approximately $0.02U_\infty D$ at a distance D from the leading edge. This volume-flow rate is equivalent to an injection velocity $U_i = 0.02U_\infty$, and hence it would certainly be expected that viscous effects will dominate when $B \approx 0.02$, and this level is indicated in figure 7. When the injection mass flow was reduced to zero, recirculation was observed within the slot

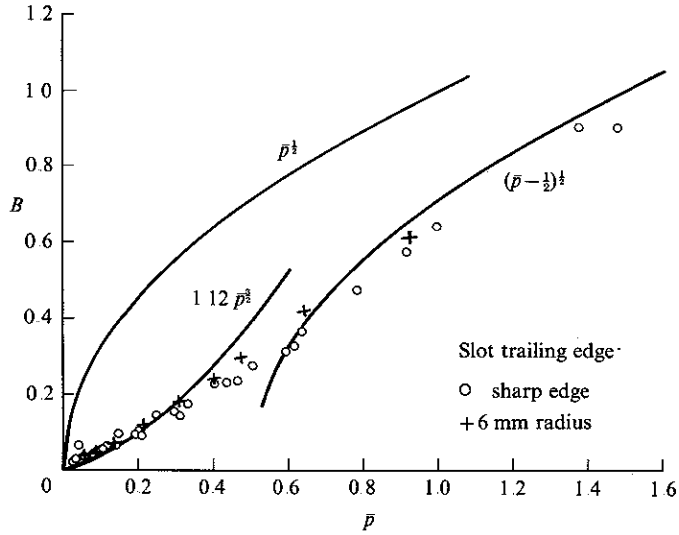

FIGURE 7 Mass-flow characteristics of the slot

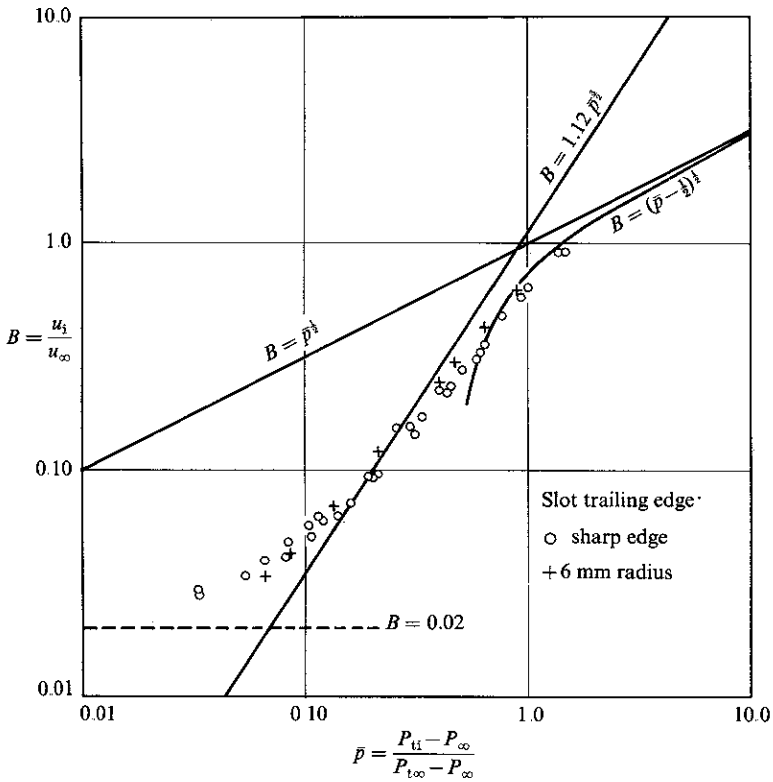

FIGURE 8 Mass-flow characteristics of the slot plotted logarithmically

passage, as would be expected. In the results presented here the upstream boundary-layer thickness was approximately $\frac{1}{10}$ of the slot width, and it should be mentioned that the mass flow from the slot increased significantly if the boundary-layer thickness was increased by a factor of three.

The presence of separation is not included in the theory, and the effect of reducing

this by slightly rounding the trailing edge of the slot was studied. The results may be seen in figures 5–8 for two radii of curvature. The pressure distributions change in the expected manner, although the effects on the mass flow characteristics are not marked.

Flow visualization of the injected gas was performed by slightly heating the injectant and allowing it to pass over a thin perspex sheet placed parallel to the tunnel sides and coated with a liquid-crystal thermochromic indicator (BDH 1984). The shape of the dividing streamline is shown in figure 9 (plate 1) for various values of B.

4. Conclusions

The theory presented in this paper represents the first attempt to quantify the effect on the flow within a slot due to the interaction between the fluid emerging from a slot and a free stream. The theory applies in the region where the injected flow remains close to the surface and yet carries significant variation in surface pressure. For a normal slot the predicted mass-flow characteristic is $B = 1.12\overline{p}^{\frac{3}{2}}$, and this has been shown to give agreement with experiment at low injection rates when separation is small. However, the injection rate must be sufficiently large for viscous interactions to be unimportant.

The picture of the flow field given by the theory is that the mainstream acts as a 'lid' over the slot, only allowing the injected fluid to escape in a region close to the rear vertex of the slot. This description is borne out by the measurements taken, the pressure within the slot being uniform and close to the injection total pressure except in the proximity of the slot's rear vertex. However, the theory clearly does not include the effects of downstream separation, upstream boundary-layer thickness or turbulent mixing downstream from the slot, but gives the correct magnitude for the mass flow properties of the slot when recovery of the mainstream against the emerging jet is dominant.

In engineering terms the analysis presented in §2 has the advantage that it may also be used, with small modifications (for full details see Fitt (1984)) when the flow is incompressible, but the densities of the free-stream fluid and the injected fluid differ. In this case it is again the pressure ratio that determines the shape of the region composed of injected fluid.

The analysis may also be capable of generalization to deal with different slot geometries, as long as the angle of injection is not too small, and it may also be possible to include the presence of a separated region downstream of the slot. One of the most important conclusions of the work described above, which was clearly evident in the experimental results, is that the flow inside the slot is dominated by the 'sink' effect at the rear vertex of the slot. A very interesting question that still remains is whether a comparable effect exists in the three-dimensional case of hole injection (see e.g. Bliss 1982), and, if so, whether the correct model consists of a single point sink at the rear vertex of the hole, or a distribution of sinks.

The authors would like to thank Drs M. Schillor and C. Please for their help with the numerical aspects of the work described above, and especially Professor D. Spence for helpful discussions and suggestions. The authors also thank Mr P. T. Ireland for his assistance in the experimental work. A. Fitt acknowledges the support of the Science & Engineering Research Council.

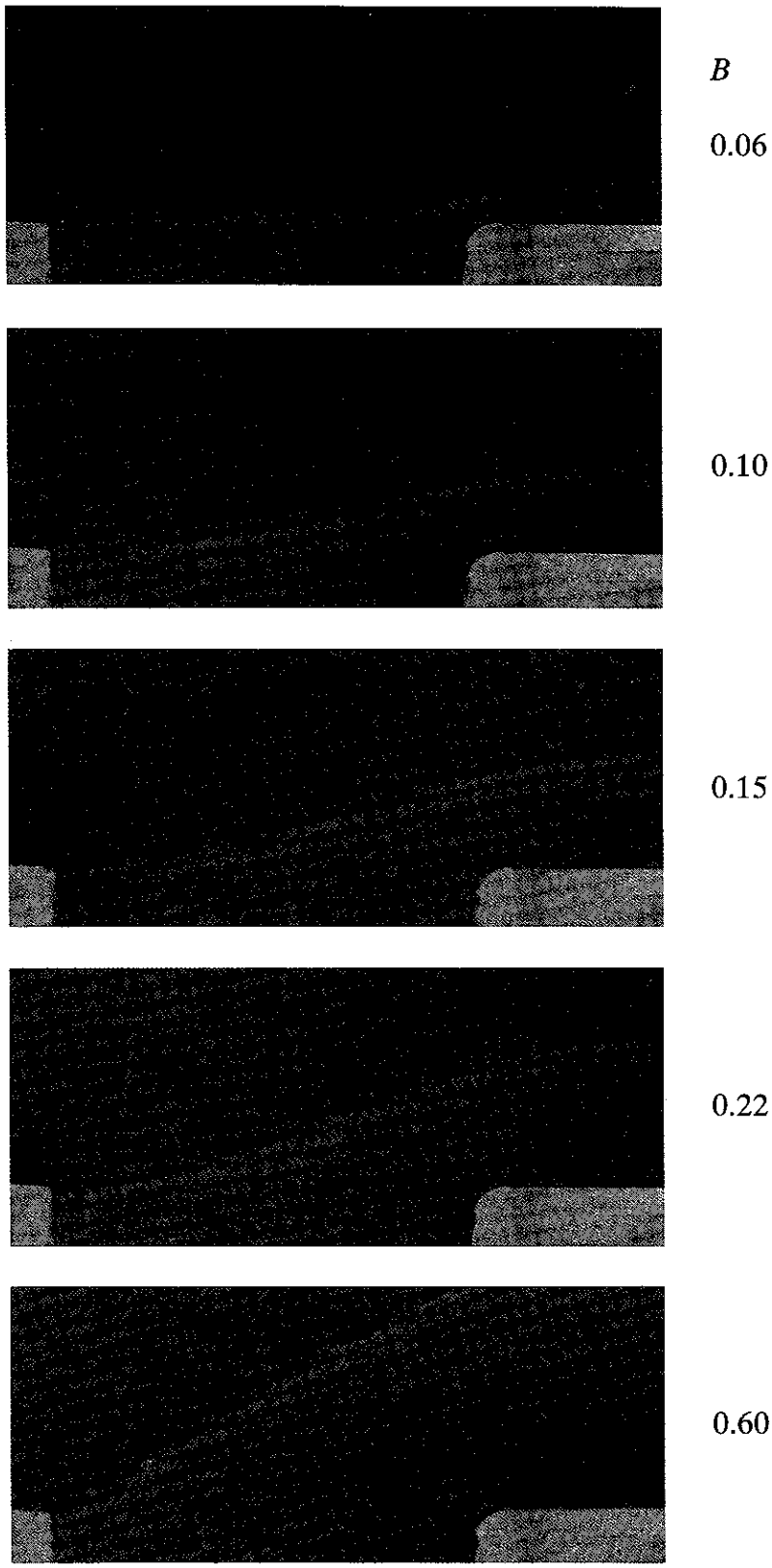

FIGURE 9. Flow visualization of the injectant using liquid-crystal thermochromic indicators.

REFERENCES

BARRY, B. 1976 The aerodynamic penalties associated with blade cooling In *Turbine Blade Cooling*; VKI LS 83.

BDH CHEMICALS LTD., POOLE, DORSET, U.K. 1984 Thermochromic liquid crystals.

BLISS, D. B. 1982 Aerodynamic behaviour of a slender slot in a wind tunnel wall *AIAA J* **20**, 1244–1252.

CHILDRESS, S. 1966 Solutions of Euler's equations containing finite eddies *Phys. Fluids* **9**, 860–872.

COLE, J. D. & AROESTY, J. 1968 The blowhard problem – inviscid flows with surface injection. *Intl J. Heat Mass Transfer* **11**, 1167–1183.

EHRICH, F. F. 1953 Penetration and deflection of jets oblique to a general stream. *J. Aero Sci* **20**, 99–104.

FITT, A. D. 1984 Theoretical aspects of film cooling. D Phil thesis, University of Oxford.

GOLDSTEIN, R. J. 1971 Film cooling. *Adv. Heat Transfer* **7**, 321–379.

MILNE-THOMSON, L. M. 1949 *Theoretical Hydrodynamics. Macmillan.*

ROSENHEAD, L. 1963 *Laminar Boundary Layers.* Clarendon.

SCHLICHTING, H. 1979 *Boundary Layer Theory* McGraw-Hill.

SMITH, F. T. & STEWARTSON, K. 1973 On slot injection into a supersonic laminar boundary layer. *Proc. R. Soc. Lond.* A **332**, 1–22.

TING, L. & RUGER, C. J. 1965 Oblique injection of a jet into a stream *AIAA J* **3**, 534–576.